

Entropy Penalty-Induced Self-Assembly in Carbon Black or Carbon Fiber Filled Polymer Blends

Guozhang Wu, Shigeo Asai, and Masao Sumita*

Department of Organic and Polymeric Materials, Tokyo Institute of Technology, 2-12-1 Ookayama, Meguro-ku, Tokyo 152-8552, Japan

Hiroshi Yui

Laboratory of Materials Science and Technology, Waseda University, 2-8-26 Nishiwaseda, Shinjuku-ku, Tokyo 169-0051, Japan

Received March 21, 2001; Revised Manuscript Received October 24, 2001

ABSTRACT: This work attempts to clarify the influence of surface roughness on the thermodynamic interactions between carbon particles and polymer melts. The surface energy of carbon black (CB) and short carbon fibers (VGCF) having different surface roughnesses was estimated by inverse gas chromatography (IGC) and highly sensitive isothermal calorimeter (HS-ITC) measurements using low-molecular-weight analogues of polymers as probes. We confirmed that the carbon surfaces possess energetic heterogeneity with the most active sites at the graphite crystalline edges, and the interactions in play are van der Waals in nature. Competitive adsorption of two chemically different polymers by incorporation of the carbon particles into the polymer blends was investigated based on SEM and TEM observations. We found that the selective location of CB in the polymer blends does not always depend on the surface tension of polymers but seems to be governed largely by the flexibility of the polymer chains. In VGCF-filled HDPE/PMMA composites, a self-assembled VGCF/HDPE network throughout the PMMA matrix was observed where the flexible HDPE chains are preferentially absorbed at the rough ends of the VGCF filaments. These experimental results lead to the conclusion that surface roughness strongly affects the carbon–polymer interactions, and the entropy penalty may play a main role in competitive adsorption of polymers on the rough carbon surfaces.

Introduction

It has been shown that polymers adsorb better on rough surfaces than on flat surfaces. The physical reason is that the entropy penalty is less for adsorption on a rough surface, if the roughness is on the scale of the polymer dimensions. This phenomenon was studied extensively^{1–5} in the past decades to understand many physicochemical applications, such as wetting, adhesion, chromatography, colloidal stabilization and biocompatibility, etc. Considerable amount of work has been devoted to properly account for the chain conformation near the surface,^{5–8} directly observe and quantitatively characterize the surface roughness,^{9–12} and prepare particles with a well-defined surface roughness.^{13,14} Nevertheless, it is still ambiguous as to what extent the polymer–surface interaction is affected by surface roughness.

Clarifying the impact of surface roughness may provide a novel way for designing supramolecular organizations. Generally, polymer adsorption takes place only when the enthalpic contribution of attractive polymer–surface contacts overcomes the loss of configurational and/or conformational entropy arising from confinement to the surface. If the entropy penalty plays a main role in determining the polymer–surface interaction, then the polymer adsorption might be controlled by surface roughness. That is to say, a rough surface may absorb a polymer when a corresponding smooth surface of the same material will not absorb. When a filler with a rough surface is incorporated into a polymer

blend, competitive adsorption of polymers may be no longer determined by the difference of chemical potentials but depends on the flexibility of polymer chains, since a flexible chain needs a low entropy cost. Actually, various kinds of the interesting possibilities have already been demonstrated by theoretical analysis and computer simulation.^{1,5,15}

In this paper, we report for the first time that carbon materials might be suitable to serve as an entropy penalty-dominating surface. Two kinds of carbon particles, that is, carbon black (CB) and a short carbon fiber named vapor-grown carbon fiber (VGCF) were used in this study. It is well-known that CB belongs to the class of rough surface materials. The roughness is from 1.0 to 100 nm, according to X-ray and recent atomic force microscopy (AFM) and scanning tunneling microscopy (STM) measurements,^{9,12} which is just on the scale from segmental size to root-mean-square radius of gyration of polymers. VGCF is a product of chemical vapor decomposition of hydrocarbons such as benzene and methane in the presence of transition metal catalysts.^{16,17} During the reaction, the hydrocarbon is adsorbed and decomposed surrounding the metal catalysts, followed by the diffusion of carbon species to the back of the catalyst particles, producing the filament structure. In the majority of cases, the catalyst particle aggregates are carried away from the surface of its support and separated from each other at the end of filaments; therefore, as shown in Figure 1, most filaments are branched at their ends. TEM and STM imaging analyses have shown that the carbon-covered ends are very rough within a range of 10 nm, while the filament body is rather smooth at that scale.^{18–20} There

* Corresponding author. Telephone: +81-3-5734-2431. Fax: +81-3-5734-2876. E-mail: msumita@o.cc.titech.ac.jp.

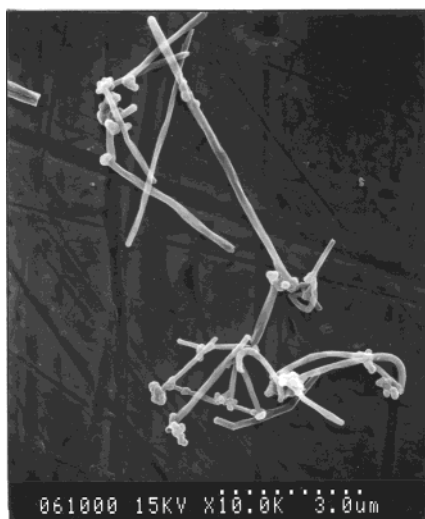


Figure 1. SEM morphology of VGCF filaments.

are many graphite crystalline edges exposed on the ends. The characteristic of VGCF, that is, having a different surface roughness between body and the ends, should be useful for clarifying the effect of surface roughness on the competitive adsorption of polymer melts.

It is worth pointing out that both of the carbon particles are often used as electrical conductive fillers. Our preliminary interest has been the design of conductive polymer composite materials by incorporation of CB or carbon fiber in immiscible polymer blends.^{21–24} The preferential adsorption of polymers on the carbon surface often leads to a heterogeneous distribution of the carbon particles in polymer matrixes and, thus, results in a very low percolation threshold. By this approach, not only does the final cost of the material decrease but also the problems caused by an excess of filler on the processing and mechanical properties of the final composites might be alleviated.^{25,26}

Experimental Section

Materials. CB (Seast 300) with a primary diameter of 28 nm and a N_2 surface area of 86 m²/g was provided by Tokai Carbon Co. VGCF with a diameter of 200 nm and an average length of 10 μ m was provided by Showa Denko Co. Both of the carbon particles were pressed under a pressure of 20 MPa, then carefully crushed and a fraction with diameters between 250 and 500 μ m was chosen by sieving. Prior to each experiment, the filler was dried at 80 °C in a vacuum oven for 24 h.

Low-molecular-weight probes used for characterization of the carbon surface were *n*-alkanes (C5–C10), benzene, formamide, and methyl acetate. These probes, having a chemical structure analogous to HDPE, PS, Nylon6, and PMMA, respectively, should closely reflect the adsorption capacity of the above polymers on the carbon surface. All probes were chromatographic-grade products and were used without further purification.

Commercial polymers with different chemical composition were used as matrixes. They are poly(methyl methacrylate) (PMMA), high-density polyethylene (HDPE), polystyrene (PS), polyamide 6 (Nylon6), poly(ethylene–vinyl acetate) (EVA with a VA content of 12%), polypropylene (PP), poly(ethyl methacrylate) (PEMA), poly(vinylidene fluoride) (PVDF), natural rubber (NR), and *trans*-polyisoprene (TPI). Some physical characteristics are shown in Table 4.

Techniques for Determination of Surface Energy. To test the effect of surface roughness on the adsorption of low-molecular-weight analogues of polymers, the surface energy of CB and VGCF was measured. There are various indirect

Table 1. Experimental Methods To Determine the Surface Energy of CB and VGCF

Mode	Zero coverage (IGC)	Limited coverage (IGC)	Equilibrium adsorption (HS-ITC)
Probe & Surface			
Equations	$\Delta G^0 = -RT \cdot \ln \frac{CV_p}{S_w}$ $\gamma_s^d = \frac{\Delta G_{CH_2}^2}{4N^2 a_{CH_2}^2 \gamma_{CH_2}}$	$\pi = RT \int_0^p q \cdot d \ln p$ $\pi = \gamma_s - \gamma_{sv}$	$\Delta H_i = -(W_i - T(\frac{\partial W_i}{\partial T}))$ $W_i = \gamma_s - \gamma_{sl}$
Probes	<i>n</i> -alkanes	<i>n</i> -octane	See Table 3

IGC: Inverse gas chromatography; HS-ITC: High-sensitive isothermal calorimeter

Table 2. Surface Energy of Carbon Particles Estimated from Different Methods

methods	unit, mJ/m ² ; data error within $\pm 5\%$			
	CB (Seast 300)		VGCF	
	γ_s^d	γ_s^p	γ_s^d	γ_s^p
IGC at zero coverage	179		119	
IGC at limited coverage	92.5		106	
HS-ITC ^a	94.5	3.6	92.1	2.6

^a The dispersive part, γ_s^d , and polar part, γ_s^p , of the surface tension were calculated from the heat of immersion based on the approach reported in ref 29. They were the average value measured by various probes, assuming that γ_s^p consists of electron-acceptor and electron-donor interactions.

methods for determining the surface free energy of a solid based on contact angles, adsorption, ζ potential, and heat of immersion measurements. The most popular methods are those based on contact angle measurements. But in the case of powders such as CB, it is rather difficult to prepare a sample with the proper surface for study; therefore, it seems that the more reliable methods are those based on adsorption and heat of immersion measurements.

The surface energy of CB and VGCF was determined using three methods as follows:

1. The first was inverse gas chromatography (IGC) measurements at zero coverage.²⁷ In this mode, the injected probe is infinitely diluted so that one may obtain the surface energy at the most active sites. *n*-Alkanes with carbon numbers from 5 to 10 were used as probes.

2. Second, IGC measurements at finite dilution mode were performed.²⁸ In this mode, measurable amounts of the *n*-octane probe were injected, leading to deformed chromatographic peaks. From the peak deformation, adsorption isotherms were obtained. By the use of the integrated form of Gibbs' adsorption equation, the spreading pressure, π , exerted by a gas adsorbed on a solid surface was calculated, and then the dispersive part of surface tension, γ_s^d .

3. Heat of immersion measurements were the final method.²⁹ By this method, the interfacial free energy was determined at equilibrium states where the carbon surface is wholly adsorbed by the probe molecules. This is different from IGC methods where the carbon surface is adsorbed in a limited coverage. Various probes including nonpolar and polar organic molecules were used so that the effect of specific interaction on adsorption energy might be distinguished.

Table 1 presents some equations for calculation of the surface tension. More details can be found in the corresponding references.

A Shimadzu GC-7A gas chromatograph equipped with a Shimadzu CR4A integrator and a flame ionization detector was used for the IGC experiments. The sized carbon particles were filled into a stainless steel column with a length of 1 m and a 2 mm inner diameter. Prior to the IGC experiment the CB filled column was heated to 200 °C under a helium flow rate of 30 mL/min for 24 h. Experiments were performed at 125

Table 3. Heat of Immersion for the Carbon Particles Adsorbed by Various Low-Molecular-Weight Probes

	surface area, m ² /g	oxygen content, wt %	unit, mJ/m ² ; data error within $\pm 2\%$				
			<i>n</i> -decane C ₁₀ H ₂₂	benzene C ₆ H ₆	methanol CH ₃ OH	formamide HCONH ₂	methyl acetate CH ₃ COOCH ₃
Seast 300	86	0.90	118	116		121	119
VGCF	12.5	0.70	119	109		117	120
BP2000 ^a	1443	1.40	98	117		113	
SAF ^b	143	1.29	117	113	122		
U-3016 ^b	91.6	0.60	119	107	111		
HAF-HS ^b	89.3	0.73	121	114	123		
SPF ^b	76.9	0.89	118	115	114		

^a Data from ref 29. ^b Data from ref 35.**Table 4. Selective Location of CB in Polymer Blends**

Polymer	<i>T_g</i> (°C)	γ_s^d	γ_p^d	γ_{CB-P} (mJ/m ²)
PMMA	105	33.2	7.9	16.5
PS	100	37.0	3.7	13.2
Nylon6	50	34.6	11.9	17.1
EVA	28	32.5	1.6	16.5
PP	-10	29.7	0.4	19.8
PEMA	-16	29.8	6.1	18.5
PVDF	-45	24.7	12.5	25.4
NR	-60	29.0	0	22.4
TPI	-65	29.0	0	22.4
HDPE	-120	35.7	0	17.6

A → B:
CB is selectively located in
B phase of A/B blends

°C with the same helium flow rate. The free energy of adsorption was calculated based on different experimental modes.

The heat of immersion for CB and VGCF was measured using a high-sensitive isothermal calorimeter (CSC 4300) at 20 °C. The carbon samples of approximately 1 g were contained in sample bulbs. They were immersed in a pocket containing a given volume of the probe liquid until adsorptive equilibrium was reached. With temperature resolution of 2 μ °C, this instrument can measure heat changes as small as 1 mcal.

Mixing Carbon Particles with Polymer Blends. Two polymers were first blended together using a two-roll mill for 5 min, followed by addition of the filler to the mixture, and mixed for 10 min. The mixing temperature was selected at which both polymers have similar viscosities. The as-produced mixtures were directly used for SEM observation, unless otherwise indicated.

Scanning Electron Microscopy (SEM) Observation. As a convenient approach to directly observe the CB–polymer interactions, the selective location of CB in two chemically different polymers was observed by means of a field emission type scanning electron microscope (FE S800, HITACHI). Specimens were fractured in liquid nitrogen. The surface of prepared specimens was etched by the Ar ion for 15 min using Eiko IB-3 equipment and coated with Pt–Pd.

Results and Discussion

Surface Energy of Carbon Particles. The surface composition of CB and VGCF has been studied by XPS.^{30,20} The oxygen content on the CB (Seast 300) surface was found to be approximately 0.9 wt %. The VGCF surface has almost the same level of oxygen content (approximately 0.7 wt %). No metal component including Fe was detected on the VGCF surface, suggesting that the metal catalyst is completely covered by the carbon species. That means the branched ends of VGCF filaments might behave like the CB particles (see Figure 1).

The surface tension of CB and VGCF measured by different methods is presented in Table 2. It is found that a different method results in a different dispersive

component of surface tension, γ_s^d . The γ_s^d decreases with increasing degree of coverage by the probes, suggesting that the carbon surface is energetically heterogeneous. The maximum value is obtained from IGC measurements at a zero coverage mode. This is reasonable because the low-molecular-weight probes first adsorb on the most active sites. The problem is which kind of site is the most active site. Wang et al.³¹ found that γ_s^d at zero coverage increases linearly with increasing specific surface area, *S*, and decreases with crystalline thickness, *L_c*, demonstrating that the most active adsorption sites might be determined by the density of graphite crystalline edges exposed on the carbon surface. Recent studies dealing with the determination of the adsorption energy distribution functions confirmed the above results.^{32,33} Computer simulations showed that the preferable adsorption of probes on the crystalline edges occurs primarily because the edges offer a highly effective adsorption area for each probe molecule. The high value of γ_s^d can thus be interpreted as a result of a low entropy loss required on the rough surface.

Note that γ_s^d of the CB particle measured at zero coverage is much higher than the value for VGCF. This should be ascribed to a higher specific surface area and a thinner crystal edge of CB. By increasing the degree of coverage by the probes, the difference reduces. The γ_s^d estimated from the immersion approach, where the carbon surface is completely covered by the probe molecules at equilibrium adsorption, should reflect the average value of samples. As listed in Table 2, the γ_s^d for CB and VGCF are 94.5 and 92.1 mJ/m², respectively. They are quite close to the surface tension of a cleaved graphite plane (90 mJ/m²) estimated from contact angle measurements.³⁴ This indicates that all of the carbon materials might have almost the same value of average surface energy.

The adsorption heat of the CB surface immersed in various probes is listed in Table 3. From the table, one can find that the heat of immersion does not change much from probe. For purpose of further confirmation, some results published in other papers,^{35,29} using various CBs having different specific surface area and oxygen content, are also listed in Table 3. All of the data show that the adsorption heat of CB is in a range from 110 to 120 mJ/m², irrespective of the nature of the carbon surface and with a variety of probe molecules. These results indicate that physical adsorption plays a main role, and van der Waals interactions between the carbon surface and the probe are much more important than dipolar-induced dipolar interactions.

The heat of immersion reflects the enthalpy contribution of probe–carbon surface interactions. Since the low-molecular-weight probes chosen for measurements have similar molecular structures as the segment of some polymers, it is expected that their results should be close

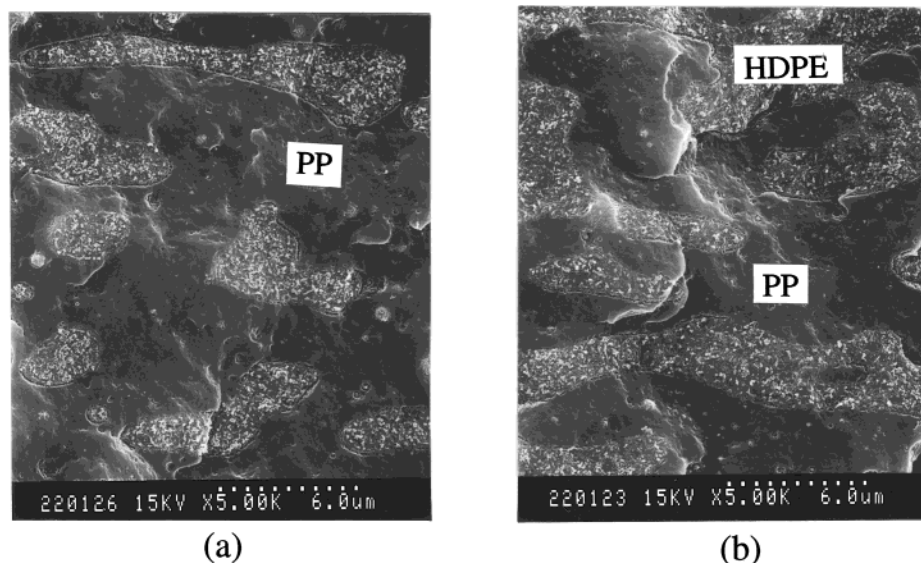


Figure 2. SEM micrographs of CB/HDPE/PP: (a) 2/30/70; (b) 2/49/49. CB is selectively located in HDPE domains as distinguished from the changes in HDPE/PP domain area.

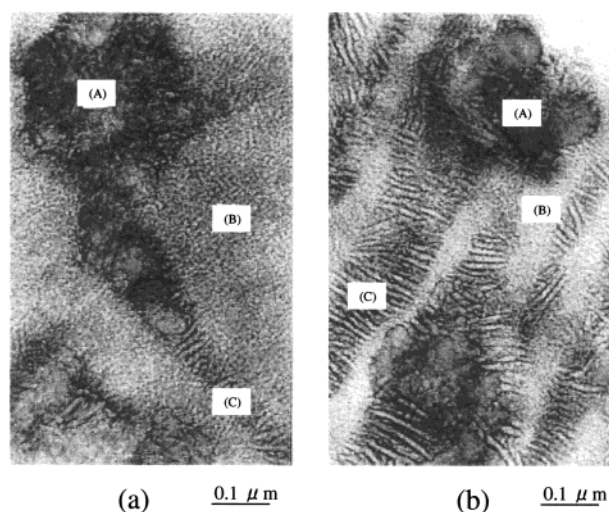


Figure 3. TEM morphology for CB/HDPE/PP by injection molding: (a) 3/10/87; (b) 5/28/67. Morphology: part A, CB-HDPE complex; part B, PP; part C, HDPE.

to the enthalpy part of interactions between these polymers and the carbon surface. The same level of enthalpy energy listed in the Table 3 hints of the importance of the entropy contribution during the competitive adsorption of polymers on the carbon surface.

Competitive Adsorption of Two Polymers on the CB Surface. Figure 2 shows typical SEM micrographs for CB/HDPE/PP composites prepared from two-roll mixing. From the change in ratios of the HDPE/PP domain area in Figure 2a and Figure 2b, one can distinguish that the CB particles are selectively located in HDPE domains. Figure 3 shows TEM pictures for the CB/HDPE/PP mixtures by injection molding at a high shear rate under high pressure (injection temperature 240 °C and injection pressure 400 kg/cm²). We observed that the morphology always consists of three parts: (A) CB-HDPE complex; (B) free PP domain (thin lamella part); (C) free HDPE domain (thick lamella part). CB particles are always surrounded by the HDPE lamella and the CB network is self-organized along the HDPE domains. It has been reported recently that HDPE/PP

might become a miscible polymer blend at a high shear rate.³⁶ The fascinating structure in Figure 3 could arise from the phase separation of the HDPE/PP blend when the high shear rate condition was removed.^{36,37}

A variety of polymer pairs with different surface tensions and glass transition temperatures were blended with the same kind of CB (Seast 300). To alleviate the influence of mixing conditions on CB location and also for a better distinction of CB location, experiments were strictly controlled under the following procedures. (1) Two polymers were first blended sufficiently using a two-roll mill, and then CB was added. The blend ratios for each pair of polymers were 70/30, 50/50 and 30/70, and the CB concentration was as low as possible (about 2 phr (per hundred parts of matrix)). (2) The mixing temperature was selected so the viscosities of the blending polymers were comparable such that the influence of viscosity on the CB location might be limited. (3) The as-mixed composites were directly used for SEM observation so as to limit the transfer of CB to the interface region during the coalescence of polymer domains.

The results are summarized in Table 4. The symbol $A \rightarrow B$ in this table means that polymer A is blended with polymer B and CB particles are selectively located in the B phases. For example, CB is selectively located in the HDPE phase of PMMA/HDPE blend as shown in Table 4. The surface tension, γ_p^d and γ_p^p , and the glass transition temperature (T_g) of polymers listed are obtained from refs 39 and 40.

Generally, competitive adsorption of polymer melts on a solid surface is determined by the CB-polymer interaction. When CB particles mixed with a polymer blend consisting of polymers A and B, the location of CB should be predicted by Young's equation³⁸

$$\omega = \frac{(\gamma_{CB-A} - \gamma_{CB-B})}{\gamma_{A-B}} \quad (1)$$

where γ_{CB-A} , γ_{CB-B} , and γ_{A-B} are, respectively, the interfacial energy between polymer A and CB, between polymer B and CB, and between polymers. The inter-

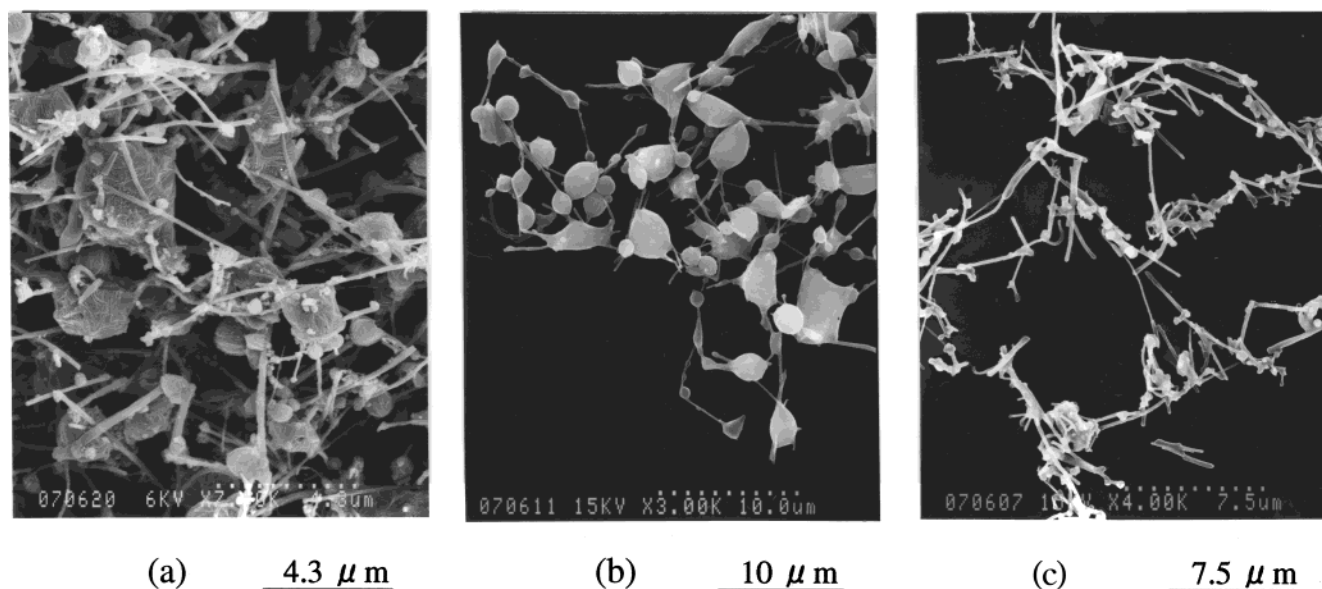


Figure 4. SEM micrographs of PMMA-extracted VGCF/HDPE/PMMA composites: (a) VGCF/HDPE/PMMA(2.5/5/95); (b) 1.5/5/95; (c) 4/1/99.

facial energy can be calculated from³⁹

$$\gamma_{12} = [(\gamma_1^d)^{1/2} - (\gamma_2^d)^{1/2}]^2 + [(\gamma_1^p)^{1/2} - (\gamma_2^p)^{1/2}]^2 \quad (2)$$

CB particles are expected to be selectively located in one of two polymer phases where the polymer has a higher interaction with the CB surface: $\omega > 0$, that is, $\gamma_{CB-A} > \gamma_{CB-B}$, CB particles in polymer B or at the interface; $\omega < 0$, that is, $\gamma_{CB-A} < \gamma_{CB-B}$, CB particles in polymer A or at the interfaces.

Let us compare the theoretical predictions with our experimental results shown in Table 4. The interfacial energy between CB and polymer, γ_{CB-p} , listed in Table 4, was calculated from eq 2 using $\gamma_{CB}^d = 94.5 \text{ mJ/m}^2$ and $\gamma_{CB}^p = 3.6 \text{ mJ/m}^2$. From the table, we find that the selective location of CB particles seems neither dependent on γ_{CB-p} nor related to the surface tension of polymers, but it directly corresponds to the glass transition temperature, T_g . CB is preferentially dispersed in a polymer with a lower T_g , except for the CB/HDPE/Nylon6 mixture. These results strongly suggest that Young's equation is not suitable for predicting the location of CB in polymer blends.

Actually, the adsorption of polymer chains on a solid surface will inevitably reduce the conformation number. If this can be regarded as a reduction of entropy, the reduction is different between two chemically different polymers. Many experimental results^{5,39} have shown that when a solid surface is regular (smooth, homogeneous, planar, and nondeformable) and there exists strong specific interactions between the surface and the polymer, the difference of the entropy for two polymers is negligible. Young's equation is hereby deduced assuming that the difference of adsorption enthalpy between two polymers is much larger than that of entropic loss

$$|\Delta H_{CB-A} - \Delta H_{CB-B}| \gg T|\Delta S_{CB-A} - \Delta S_{CB-B}| \quad (3)$$

where ΔH_{CB-A} and ΔH_{CB-B} are the adsorption enthalpies and $T\Delta S_{CB-A}$ and $T\Delta S_{CB-B}$ are the adsorption entropic losses of polymers A and B on CB surfaces.

However, these conditions cannot be satisfied by the CB surface. CB particles have a fractal surface.^{4,9,12} Their roughness is given on a nanometer scale from 1.0 to 100 nm, which is just on the scale from segment size to root-mean-square radius of gyration of a polymer. Our IGC results showed that CB has a surface with energetic heterogeneity, and the most active sites are graphite edges. As a consequence, polymer chains will preferentially be adsorbed along the edges of the crystal. This may greatly reduce the entropic loss and result in a better adsorption, on one hand; however, on the other hand, it will enlarge the difference of the entropy (i.e., $T|\Delta S_{CB-A} - \Delta S_{CB-B}|$) if polymers with different chain flexibility are blended. More important is that there are no strong specific interactions between the CB surface and the polymers. Our results obtained from heat of immersion measurements (see Table 3) revealed that the equilibrium adsorption heat measured by chemically different probes is very close within a range from 110 to 120 mJ/m^2 , suggesting that the difference of the adsorption enthalpy ($\Delta H_{CB-A} - \Delta H_{CB-B}$) between two polymers is rather small.

On the basis of the two aspects above, we believe that the difference in entropy loss between two polymers may play a main role in competitive adsorption of polymers on CB surfaces. Our results that CB is selectively located in a polymer with a lower T_g should arise from this source. Because, for polymers having a similar carbon-carbon main chain, a lower T_g is generally related to a higher flexibility of chains and thus a low entropic loss for adsorption on the CB surface. It should be pointed out that the T_g value is not always correlated to chain flexibility, especially when the comparison is between two different kinds of main chains such as HDPE and polyamide. An exception of Nylon6 blended mixtures could be ascribed partially to this reason.

Competitive Adsorption of Polymers on VGCF Filaments. It is of great interest to directly observe the effect of surface roughness on the competitive adsorption of polymers using a carbon filament having different surface roughness between the body and the end. Figure 4a shows the morphology of VGCF/HDPE/PMMA composites containing 5 wt % HDPE (weight percent of total

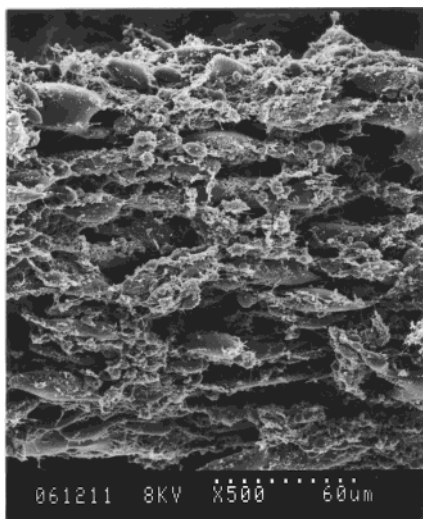


Figure 5. SEM micrograph of PMMA-extracted VGCF/HDPE/PMMA composite containing 20 wt % HDPE and 2.5 phr VGCF.

polymer matrix) and 2.5 phr VGCF. Figure 4b shows the SEM picture for the mixture filled with 1.5 phr VGCF whereas Figure 4c is for the mixture containing 1 wt % HDPE and 4.0 phr VGCF. Here, the PMMA was first mixed with HDPE using a two-roll mill at 220 °C for 5 min, followed by addition of VGCF to the mixture and mixed for 10 min. To clarify the HDPE domain in these pictures, PMMA has been selectively extracted by chloroform at room temperature for 72 h. It is clearly observed that the HDPE domains are separated from each other and preferentially adsorbed at the end parts of VGCF filaments, even if the content of HDPE is as low as 1 wt % (see Figure 4c) or the concentration of VGCF reduced to 1.5 phr (see Figure 4b). A study of electrical conductivity in our previous communication²¹ showed that the percolation threshold of VGCF/PMMA composites can be reduced remarkably from 8.0 phr to 1.5 phr with addition of only 1 wt % HDPE. These results strongly suggest that a novel self-assembled electrical network is constructed in VGCF/HDPE/PMMA composites due to the preferential adsorption of the HDPE domains at the ends of VGCF filaments.

Figure 5 shows the morphology of VGCF/HDPE/PMMA where the content of HDPE is increased to 20 wt %. Two groups of HDPE domains with different size are observed. Many filaments are pulled out from large HDPE domains forming the VGCF/HDPE self-assembled architecture throughout the PMMA matrix. It appears that the body of VGCF filaments is preferentially adsorbed by PMMA.

With regard to the question why HDPE is selectively located at the ends of VGCF rather than coating the whole length of the fiber, three aspects have been thoroughly considered. One possibility is that VGCF has a chemically different surface between the body and the end, for example, exposing the metal catalyst at the end. However, XPS studies did not confirm this possibility. Furthermore, the surface energy of VGCF determined at zero coverage, which should represent the most active adsorption site on the VGCF surface, is about 119 mJ/m² (see Table 2). This value is quite close to the value of graphite particles.³¹

Another possibility might be the effect of capillarity.^{39,41} This effect has been frequently applied to account for the relative motion between a solid and a

liquid. When two filaments move together and cross over, the capillary force may drive HDPE melts to the confined space causing selective adsorption of HDPE at a cross over part of VGCF. However, if this is true, PMMA may also selectively locate at the end of VGCF when the content ratio of HDPE/PMMA is 95/5. We did not observe this phenomenon even when the PMMA viscosity is very low.

The most reasonable possibility might be the effect of difference in geometric heterogeneity between the body and the end of the filaments. At the ends, most of the filaments are branched and expose many carbon crystallite edges, resulting in a rough surface like CB particles. Therefore, like carbon black which always selectively locates in the HDPE phase in HDPE/PMMA blends,³⁸ HDPE is preferentially adsorbed at the ends of the filaments due to the effect of an entropy penalty. However, at the filament body, the situation changes. The VGCF body is rather smooth. This inevitably alleviates the difference in entropy variation between two polymers, and, as a result, the high-polarity PMMA matrix is preferential for adsorption of the VGCF body instead of nonpolar HDPE.

Conclusions

Carbon particles have an energetically heterogeneous surface. The most active sites were believed to be at the graphite crystallite edges, a primary composition leading to the roughness of the carbon surface. We further confirmed that the specific interactions of the carbon particles are very weak.

The selective location of CB in two chemically different polymer melts is not always determined by the surface tension of polymers. In many cases, it is governed by the flexibility of polymer chains. These results suggest that the entropy penalty may play a main role in competitive adsorption of polymers on the CB surfaces.

Change in the surface roughness of the carbon particles may control the preferential adsorption of polymers. A typical example is VGCF-filled HDPE/PMMA composites. We find that the HDPE chains are preferentially adsorbed at the rough ends of filaments, resulting in a self-assembled VGCF/HDPE network in a PMMA matrix.

References and Notes

- (1) Douglas, J. F. *Macromolecules* **1989**, *22*, 3707.
- (2) Blunt, M.; Barford, W.; Ball, R. *Macromolecules* **1989**, *22*, 1415.
- (3) Baumgartner, A.; Muthukumar, M. *J. Chem. Phys.* **1991**, *94*, 4062.
- (4) Heinrich, G.; Vilgis, T. A. *Macromolecules* **1993**, *26*, 1109.
- (5) Fleer, G. J.; Cohen Stuart, M. A.; Scheutjens, J. M. H. M.; Cosgrove, T.; Vincent, B. *Polymers at Interface*; Chapman & Hall: London, 1993.
- (6) de Gennes, P. G. *Macromolecules* **1980**, *13*, 1069.
- (7) Dimarzio, E. A. *J. Chem. Phys.* **1965**, *42*, 2101.
- (8) Smith, G. D.; Yoon, D. Y.; Jaffe, R. L. *Macromolecules* **1992**, *25*, 7011.
- (9) Donnet, J.-B.; Wang, T. K. *Macromol. Symp.* **1996**, *108*, 97.
- (10) Hoffman, W. P.; Fernandez, M. B.; Rao, M. B. *Carbon* **1994**, *32*, 1383.
- (11) Avnir, D.; Pfeifer, P.; Farin, D. *J. Chem. Phys.* **1983**, *79*, 3566.
- (12) Donnet, J.-B. *Rubber Chem. Technol.* **1998**, *71*, 323.
- (13) Luchow, H.; Breier, E.; Gronski, W. *Rubber Chem. Technol.* **1997**, *70*, 747.
- (14) Pignataro, B.; Bonis, A. D.; Compagnini, G. *J. Chem. Phys.* **2000**, *113*, 5947.
- (15) Kummer, S. K.; Russell, T. P. *Macromolecules* **1991**, *24*, 3816.

- (16) Koto, T.; Haruta, K.; Kusakabe, K.; Morooka, S. *Carbon* **1992**, *30*, 989.
- (17) Downs, W. B.; Baker, R. T. K. *Carbon*, **1991**, *29*, 1173.
- (18) Endo, M.; Takeuchi, K.; Kobori, K.; Takahashi, K.; Kroto, H. W.; Sarkar, A. *Carbon* **1995**, *33*, 873.
- (19) Oberlin, A.; Endo, M.; Koyama, T. *J. Cryst. Growth* **1976**, *32*, 335.
- (20) Darmstadt, H.; Roy, C.; Kaliaguine, S.; Ting, J.-M.; Alig, R. L. *Carbon* **1998**, *36*, 1183.
- (21) Wu, G.; Asai, S.; Sumita, M. *Macromolecules* **1999**, *32*, 3534.
- (22) Wu, G.; Miura, T.; Asai, S.; Sumita, M. *Polymer* **2001**, *42*, 3271.
- (23) Wu, G.; Asai, S.; Zhang, C.; Miura, T.; Sumita, M. *J. Appl. Phys.* **2000**, *88*, 1480.
- (24) Sumita, M.; Sakata, K.; Hayakawa, Y.; Asai, S.; Miyasaka, K.; Tanemura, M. *Colloid Polym. Sci.* **1992**, *270*, 134.
- (25) Gubbels, F.; Blacher, S.; Vanlathem, E.; Jerome, R.; Deltour, R.; Brouers, F.; Teyssie, Ph. *Macromolecules* **1995**, *28*, 1559.
- (26) Zhang, M. Q.; Yu, G.; Zeng, H. M.; Hou, Y. H.; Zhang, Y. H. *Macromolecules* **1998**, *31*, 6724.
- (27) Gilles, G. M.; Gray, D. G. *J. Colloid Interface Sci.* **1980**, *77*, 353.
- (28) Gilles, G. M.; Gray, D. G. *J. Colloid Interface Sci.* **1979**, *71*, 93.
- (29) Gonzalez-Martin, M. L.; Janczuk, B.; Labajos-Broncano, L.; Bruque, J. M. *Langmuir* **1997**, *13*, 5991.
- (30) Asai, S.; Sakata, K.; Sumita, M.; Miyasaka, K.; Sawatari, A. *J. Chem. Soc. Jpn., Chem. Ind. Chem.* **1991**, *12*, 1672.
- (31) Wang, M.-J.; Wolff, S. *Rubber Chem. Technol.* **1991**, *64*, 559.
- (32) Papirer, E.; Brendle, E.; Ozil, F.; Balard, H. *Carbon* **1999**, *37*, 1265.
- (33) Barad, H. *Langmuir* **1997**, *13*, 1260.
- (34) Donnet, J.-B. *International Symposium On Carbon*; Toyohashi, Japan, The Society of Polymer Science: Tokyo, Japan, 1982; pp 57–70.
- (35) Wade, W. H.; Deviney, M. L., Jr.; Brown, W. A.; Hnoosh, M. H.; Wallace, D. R. *Rubber Chem. Technol.* **1971**, *44*, 218.
- (36) Sano, H.; Yui, H.; Li, H.; Inoue, T. *Polymer* **1998**, *39*, 5262.
- (37) Yui, H.; Sano, H.; Okamura, M.; Asai, S.; Sumita, M. *Kobunshi Ronbunshu* **1996**, *53*, 745.
- (38) Sumita, M.; Sakata, K.; Asai, S.; Miyasaka, K.; Nakagawa, H. *Polym. Bull.* **1991**, *25*, 265.
- (39) Wu, S. *Polymer Interface and Adhesion*; Marcel Dekker: New York, 1982.
- (40) Ferry, J. D. *Viscoelastic Properties of Polymers*; John Wiley & Sons: New York, 1970.
- (41) Dyba, R. V.; Miller, B. *Text. Res. J.* **1969**, *39*, 962.

MA0104940